Article

Spatiotemporal Variability, Trends, and Potential Impacts of Extreme Rainfall Events in the Sudano-Sahelian Region of Cameroon

Ibrahim Njouenwet [1,*], Lucie Angennes Djiotang Tchotchou [1], Brian Odhiambo Ayugi [2,3], Guy Merlin Guenang [4], Derbetini Appolinaire Vondou [1] and Robert Nouayou [5]

1   Laboratory of Environmental Modeling and Atmospheric Physics, Department of Physics, University of Yaounde 1, Yaoundé P.O. Box 812, Cameroon
2   Department of Civil Engineering, Seoul National University of Science and Technology, Seoul 01811, Korea
3   Organization of African Academic Doctors (OAAD), Off Kamiti Road, Nairobi P.O. Box 25305-00100, Kenya
4   Department of Physics, Faculty of Science, University of Dschang, Dschang P.O. Box 96, Cameroon
5   Laboratory of Geophysics and Geoexploration, Department of Physics, University of Yaounde 1, Yaoundé P.O. Box 812, Cameroon
*   Correspondence: njouenwetibrahim@yahoo.fr

Abstract: The Sudano-Sahelian region of Cameroon is mainly drained by the Benue, Chari, and Logone rivers; which are very useful for water resources; especially for irrigation, hydropower generation, and navigation. Long-term changes in mean and extreme rainfall events in the region may be of crucial importance in understanding the impacts of climate change. Daily and monthly rainfall data from fifteen climate stations in the study area from 1980 to 2018 and measurements from the Expert Team on Climate Change Detection and Indices (ETCCDI) were estimated using the non-parametric innovative trend analysis (ITA) and the Sen slope estimator. The precipitation concentration index (PCI), the precipitation concentration degree (PCD), and the precipitation concentration period (PCP) were used to explore the spatiotemporal variations in the characteristics of rainfall concentrations. The results showed complex spatial patterns of the annual average PCI values across the Sudano-Sahelian region; which varied from values lower in the south to higher in the far north, which were the characteristic of seasonality and a strong seasonal precipitation distribution throughout the year; respectively. The PCD results revealed that the annual rainy days in a year decreased from the south to the far north. Additionally, the PCP results indicated a slightly later occurrence of precipitation. A significant trend toward more intense–extreme rainfall events was observed in most parts of the study area, but a significant trend toward more humid days was observed in the southeastern part. Trends in dry days significantly increased in the central and southwestern parts of the study area. This could mean that the prevalence of flood and drought risks are higher in the study area. Overall, the increase in annual rainfall could benefit the hydro-power sector, agricultural irrigation, the availability of potable water sources, and food security.

Keywords: extreme precipitation indices; Sudano-Sahelian regions; precipitation; irrigation; food security

1. Introduction

The Sahelian region has been identified as having the highest rainfall variability in the world in the last century [1]. Subsequently, it is one of the world's largest semi-arid regions, where income sources are mainly based on rain-fed agriculture and animal husbandry [2]. However, the authors of [3,4] have noted that, in the 21st century, climate change will negatively influence established resilience in the area, not only by increasing the year-to-year variability of rainfall patterns but also by increasing unpredictable seasonality and the number of heavy rainfall events and droughts [5,6]. The beginning (and lengths) of the

dry and wet seasons, as well as the amount of annual rainfall, vary across the region [7]. However, agricultural crops are closely linked to factors, such as water availability and seasonal parameters (onset and retreat dates) [8,9]. Predominantly, the economies of West African countries, including the Sahelian regions, are directly affected via agriculture, which is essentially rainfed, poor water quality, and poor management of water reservoirs for hydroelectric dams and irrigation [7]. However, data from stations in West Africa, particularly the Sahel, are missing due to different policies in different countries [10]. For this reason, an Intergovernmental Panel on Climate Change special report on extreme events [4] has highlighted the lack of studies on regional variability and trends in extreme rainfall and drought due to lack of data.

The Sudano-Sahelian region is the area's highest population density and the most vulnerable to climate change, particularly the Cameroon region [11]. In terms of administration, it includes the far north and the northern regions and accounts for over one-fifth of Cameroon's total territory. The far north region has 74.3% of the population living below the poverty line [12]. Subsistence agriculture (rainfed, irrigated) accounts for 65% of the region's economic activity [13]. The Sudano-Sahelian region holds a strategically important position in Cameroon's economic development due to its vast area and water resources, which are the major sources of electricity via hydropower plants, high agricultural productive potential, and nomadic animal husbandry. The Benue and Logone-Chari Rivers are the main streaming sources in the Sudano-Sahelian region of Cameroon, which extends from the Adamawa region in the south through Nigeria to the Niger River in the west, and from Lake Chad in the north to Chad and Central Africa republic in the south of the study area, respectively. The Benue River also feeds the Lagdo Reservoir. the Lagdo Dam on the river Benue, with a useful capacity of close to 6 billion m^3; it is the only classical multipurpose dam in Cameroon because it facilitates, at the same time, the hydro-electricity production with a capacity of 84 MW, irrigation plantation of 80,000 ha, and the river regulation for navigation [14]. Thus, the rainfall distribution caused by climate change may severely affect the water cycle and food security in the Sudano-Sahelian region of Cameroon.

From September 1982 to 2000, the Sudano-Sahelian region of Cameroon suffered from extreme climate events, such as droughts, causing considerable impacts on the country's environment, human activities, and economy [15]. For instance, the September 2012 floods in Maga and Yagoua resulted in many lives being lost while others were displaced, and the main hospital and other public infrastructures were destroyed due to heavy rainfall [16,17]. During that same year, a serious threat to food security was reported in more than half of the administrative units; more than 14,000 hectares of crops (e.g., 12,000 hectares of cotton—6% of cotton crops cultivated—and 12,375 fruit plants) were destroyed (Ministry of Agriculture and Rural Development, 2012). Reference [18] showed that water resources vary with the changing climatic conditions and the severity of the impacts vary from region to region. As such, local studies are essential to analyze the changes in precipitation extremes.

Several studies have assessed the spatiotemporal trends in mean and extreme rainfall events across West Africa [10,19,20], including the Sudano-Sahelian regions due to global warming. Most of these studies observed increasing trends in the annual mean rainfall and extreme events from 1980 to 2010. Likewise, regarding Central Africa, reference [21] projects increasing trends of heavy rainfalls over Sudano-Sahelian, Cameroon, by 2100. However, most of these studies are limited in their assessments to specific regions, i.e., they are 'delimited' by the lack of station data in West Africa, especially the Sudano-Sahelian region of Cameroon.

At the local scale, only two studies have been conducted. Reference [22] analyzed long-term trends in the mean and climate variabilities (only rainfall) over the study area and found that at the 95% level of confidence, 10% of stations displayed statistically significant decreases while 5% of stations showed statistically significant increases using a homogeneous monthly and annual rainfall database of twenty-five stations located in northern Cameroon. In [23], the authors examined the extremes for the whole area of Cameroon, including the Sudano-Sahelian region. The differences with the current studies

are (1) the use of a different set of stations, (2) the current study examines only the Sudano-Sahelian part of Cameroon, (3) the PCI, PCP, and PCD analyses, and (4) the methods (regarding extreme rainfall) used in this study included the innovative trend analysis (ITA) originated by [24–26]. Based on the findings of the tests and their performances, [27] found that the ITA test appeared to be the best trend detection technique among the four techniques of the Mann–Kendall test family [28,29]. As such, on a local scale, this study is unique in terms of its use of station density, comprehensive assessment of trends, and changes in rainfall, variability, and extreme events.

Accordingly, the objectives of this study were to fill this gap of data and extend the work of [10,19,20] in the Sahel West Africa by performing a more comprehensive assessment of the spatial variability and trends in the rainfall amounts and extremes using four decades of station data, with stations distributed throughout the Sudano-Sahelian area of Cameroon. Such information is important for decision-makers and farmers to address climate change through sustainable adaptation strategies. The rest of this paper is organized as follows: section two describes the study area, data, and methods, while section three presents the results and discussion. The final section presents the conclusion of the study.

2. Study Area, Data, and Method

2.1. Study Area and Data

The Sudano-Sahelian region lies between 7° N and 13° N longitude and 11.5° E and 16° E latitude (Figure 1). It is a relatively flat topography. It has a drainage area of about 100,000 km^2 with a population of about 5,530,643 inhabitants. It is located in the north of Cameroon and covers two administrative regions (the far north and north). The Sudano-Sahelian region has geostrategic importance as a source of water resources, a potential for hydropower, and is favorable to the livestock and growth of cotton, millet, sorghum, maize, rice, groundnuts, and onions. All of these crops are supervised by major companies, such as "Société de Développement du Coton (SODECOTON)" and "Société d'Expansion et de Modernisation de la Riziculture dans la ville de Yagoua (SEMRY)". The climate of the study area can be broadly divided into two: the Sahelian and Sudanian zone located northward and southward of 9° N, respectively. Generally, the climate is under the influence of the thermodynamic properties of the African Monsoon, which brings rain between June and September in the Sahelian zone and May and October in the Sudanian zone. The annual rainfall increases from the north toward the south between 328 and 1670 mm. This area is under the strong influence of humidity advected from the Atlantic Ocean and from southwesterly [30]. The daily temperatures are usually between 25 and 34 °C.

Datasets used in this work were daily and monthly rainfalls from 15 stations across the Sudano-Sahelian region of Cameroon for the 39-year period. This dataset was collected from the support services of SODECOTON. The locations are shown in Figure 1 and described in Table 1.

2.2. Method

2.2.1. Statistical Test of Homogeneity

Data homogeneity was first tested using the standard normal homogeneity test (SNHT) for a single break [31], the Buishand range test [32], the Pettitt test [33], and the Von Neumann ratio test [34] at 1% significance levels. Three of the four tests were used to determine the years of a break (location-specific tests) while the Von Neumann ratio test (non-specific location) did not specify the year of the rupture but rather a value that, when compared with a threshold set in relation to the number of years used in the test, indicated whether the null hypothesis was rejected or not. The analysis was based on four tests, including three possible results that depended on the number of tests rejecting the null hypothesis (breakpoint): zero or one test that rejected this hypothesis (useful), two tests (doubtful), and three tests (suspect). The test variable was the annual rainfall. In the following, when a station is labeled either useful or doubtful it may be used for trend

analysis and variability; when it is labeled suspect, it lacks credibility. Details on the descriptions of these four methods can be found in [35].
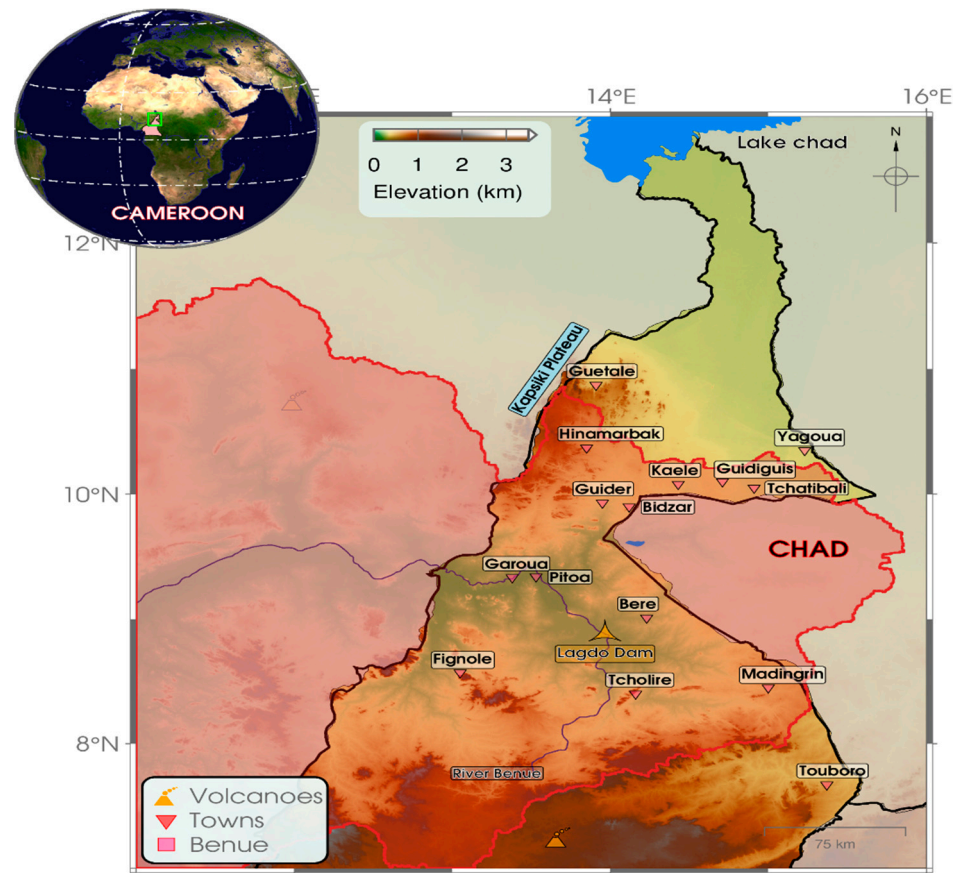
Figure 1. Map of the study area with the Sudano-Sahelian political border of Cameroon, topography and selected rainfall stations. Red line delineates the water catchment boundary.

Table 1. Geographical descriptions of the data, altitude, period of measurement, and percentage of missing data.

Stations	Latitude (°N)	Longitude (°E)	Altitude (m)	Period	Annual Rainfall (mm)	Max (mm)	Min (mm)	Standard Deviation	Missing (%)
Bidzar	9.9	14.12	470	1980–2019	883.6	1319	534.9	183.5	1.8
Fignole	8.57	13.05	523	1980–2019	1178	1654	688	221.6	0
Guetale	10.07	13.91	490	1980–2019	794.6	1013	436	135.2	2.8
Guider	9.03	13.95	356	1980–2019	891	1212	557	171.9	2.8
Guidiguis	10.10	14.71	362	1980–2019	779.9	1077	597	138.2	0.8
Hina-Marbak	10.37	13.85	544	1980–2019	945	1260	554.2	168.1	0.8
Kaélé	10.08	14.43	388	1980–2019	823.9	1080	604.7	151.7	0
Pitoa	9.34	13.53	274	1980–2019	926.7	1304	387	182.2	0
Tchatibali	10.05	14.91	815	1980–2019	820.9	1162	491	169.1	0
Touboro	7.67	15.37	500	1980–2019	1248	1539	830	195.9	0.6
Yagoua	10.35	15.23	325	1980–2019	715.9	1044	110	170.3	0
Bere	9.01	14.23	238	1980–2018	954.6	1258	554	176.3	0
Garoua	8.56	13.05	213	1980–2018	981.6	1258	554	194.8	0.8
Madingring	8.45	15.00	430	1980–2018	1094	1336	660	170.1	0
Tchollire	8.4	14.16	392	1980–2018	1209	1670	736	208.9	1.7

2.2.2. Precipitation Concentration Index

The PCI is a powerful indicator of rainfall concentration, droughts, flood risk prediction, and soil erosivity for annual and seasonal scales (wet and dry seasons) [36]. PCI was calculated on the annual and seasonal scales for each climate station. The PCI for a given data series station can be calculated as below,

$$PCI_{annual} = \frac{\sum_{i=1}^{12} P_i^2}{(\sum_{i=1}^{12} P_i)^2} \tag{1}$$

$$PCI_{wet} = \frac{\sum_{i=1}^{nw} P_i^2}{(\sum_{i=1}^{nw} P_i)^2} \frac{100 \times nw}{12} \tag{2}$$

$$PCI_{dry} = \frac{\sum_{i=1}^{nd} P_i^2}{(\sum_{i=1}^{nd} P_i)^2} \frac{100 \times nd}{12} \tag{3}$$

where P_i is the monthly amount of rainfall in month i, calculated for each climate station. The seasonal PCI_{dry} and PCI_{wet} were computed on a seasonal scale based on the dry season from October to May and the wet season from June to September; nw and nd represent, respectively, the number of rainy and dry season months.

As defined in the classification range of PCI values, i.e., [37], the rate of positive values of PCI, ≤ 10, is termed as a uniform distribution (i.e., low precipitation concentration); $10 < PCI \leq 15$ refers to moderate precipitation distribution; $16 < PCI \leq 20$ refers to irregular precipitation distribution, and $PCI > 20$ describes strong irregularity of precipitation distribution.

2.2.3. Calculation of PCD and PCP

The PCD and PCP were proposed by [38] to measure the distribution of rainfall and the month in which total precipitation concentrated, respectively. They showed that the length of the rainy season or the number of rainy days was inversely related to the PCD value. The PCD and PCP were basically developed on the assumptions that the total monthly precipitation is a vector containing both magnitudes and directions. These represent, respectively, the amount of precipitation in each month and the angles assigned to each month in 30° steps running from 0 to 360° for a year. They can be defined as below:

$$\theta_j = \frac{360 \times j}{n} \tag{4}$$

$$R_i = \sum r_{ij} \tag{5}$$

$$R_{xi} = \sum_{j=1}^{N} r_{ij} \times \sin \theta_j \tag{6}$$

$$R_{yi} = \sum_{j=1}^{N} r_{ij} \times \cos \theta_j \tag{7}$$

$$PCD_i = \frac{\sqrt{R_{xi}^2 + R_{yi}^2}}{R_i} \tag{8}$$

$$\alpha_i = \tan^{-1}\left(\frac{R_{xi}}{R_{yi}}\right) \tag{9}$$

$$PCP_i = \alpha_i \times \left(\frac{n}{360}\right) \tag{10}$$

where i is the year (i = 1980, 1981, ... , 2018), and R_i is the amount of rainfall of a year. j is the month (j = 1, 2, ... , 12) and n is the number of month per year. θ_j represents the corresponding azimuth angle of the jth month, while the year can be seen as 360°. r_{ij} represents the precipitation of the jth month in the ith year.

2.2.4. Precipitation Indices

Ten indices of extreme precipitation defined by the Expert Team on Climate Change Detection and Indices (ETCCDI) were considered [39], and calculated using the RClimDex model (Table 2).

Table 2. Definition of ETCCDI indices based on daily precipitation and units.

Variables	Description	Definitions	Units
cdd	Consecutive dry days	Maximum number of consecutive dry days	days
cwd	Consecutive wet days	Maximum number of consecutive wet days	days
r10	Number of heavy precipitation days	Annual count of days when RR $\geq$ 10 mm	Days
r25	Number of very heavy precipitation days	Annual count of days when RR $\geq$ 25 mm	Days
ptot	Annual precipitation	Annual total precipitation when RR $\geq$ 1 mm	mm
r95p	Very wet days	Annual total precipitation when RR > 95th percentile	mm
r99p	Extremely wet days	Annual total precipitation when RR > 99th percentile	mm
rx1day	Maximum 1 day of precipitation	Annual highest daily precipitation	mm
rx5day	Maximum 5 days of precipitation	Annual highest 5 consecutive days of precipitation	mm
sdii	Simple daily intensity index	Annual precipitation divided by number of wet days	mm/day

Reference [39] classified the extreme precipitations into three groups: (1) intensity indices (mm): annual total wet-day precipitation (PRCPTOT), very wet days (R95p), extremely wet days (R99p), highest 1-day precipitation in a year (Rx1d), highest 5-day precipitation in a year (Rx5d), and simple daily intensity index (SDII, mm/day); (2) frequency indices (days): number of heavy precipitation days (R10mm) and number of very heavy precipitation days (R25mm); and (3) duration indices (days): consecutive dry days (CDD) and consecutive wet days (CWD).

2.2.5. The Innovative Trend Analysis

The innovative trend analysis (ITA) was applied to yield more detailed data about the overall and partial trends based on deliberate categorization in the extreme precipitation indices from 1980 to 2018. These methods were developed by [24–26] and used by researchers to increase visual properties and evaluate statistical significance [27,40]. It also provides the ability to separate low, high, and medium flow trends and their relative intensities, durations, and magnitudes. A graph that shows these possible partial trends was obtained by:

(1) Dividing the main time series into two (or more) equal sub-series,
(2) Sorting each subseries in ascending order and plotting the newest subseries on the horizontal axis against the others on the ordinate axis,
(3) Drawing a line at 1:1 (45°) and ±10% lines on the Cartesian coordinate system, which theoretically indicate that there is no trend in the given series,
(4) Classifying each group into "low", "medium", and "high" classes obtained by dividing the variation domain of the data into three equal intervals, which provide a domain of interpretation for each class of trend, which should be interpreted for the cases of "low" (future droughts) and "high" (future floods) occurrence possibilities.

In this case, the trend slope (change per unit time) was evaluated using a simple non-parametric procedure developed by [26], according to the following expression:

$$s = \frac{2(\overline{y_2} - \overline{y_1})}{n} \tag{11}$$

where n is the sample length, and $\overline{y_1}$ and $\overline{y_2}$ are the arithmetic averages of the first and second halves of a given time series, respectively.

2.2.6. Spatial Interpolation

Mean and extreme rainfalls are spatially represented using the Kriging interpolation method. The geographical information system (GIS) in R software was used for this purpose. Studies show that Kriging provides better local interpolation than other methods in the Sudano-Sahelian area of Cameroon [22,41]. As for our focus here, and given the lack of station observations, the GIS was used to fill gaps and show the spatial variability of precipitation and precipitation extremes.

3. Results and Discussions

3.1. Homogeneous Assessment

Few stations had missing values, i.e., fewer than 4% (Table 1). Homogeneity results show that 73.33% of stations were labeled as "useful", as shown in Table 3. Fignole, Guetale, Hina-Marbak, and Touboro stations were classified as "doubtful". After the homogeneity assessment, data from 15 stations should be used for the analysis of trends and variability.

Table 3. Statistical test of homogeneity applied to the annual rainfall count series of the main climate stations in the Sudano-Sahelian region of Cameroon. (*) indicates that the test rejects the null hypothesis at the 1% level and the annual data series is not homogenous.

N°	Stations	SNHT	Pettitt's Test	Buishand's Test	Von Neumann's Test	Decision
1	Bidzar	36	8	30	1.74	Useful
2	Fignole	38 *	30 *	30 *	1.58	**Doubtful**
3	Guetale	39 *	11	11	1.40 *	**Doubtful**
4	Guider	36 *	27	27	1.70	Useful
5	Guidiguis	6	6	6	2.06	Useful
6	Hina-Marbak	39 *	13	32	1.40 *	**Doubtful**
7	Kaélé	38 *	11	11	1.31	Useful
8	Pitoa	31 *	31	31	1.37	Useful
9	Tchatibali	6	14	11	1.56	Useful
10	Touboro	10 *	15 *	15 *	1.96	**Doubtful**
11	Yagoua	38	14	36	1.78	Useful
12	Bere	17	17	17	1.32	Useful
13	Garoua	8	31	8	1.68	Useful
14	Madingring	31	31	23 *	1.57	Useful
15	Tchollire	8	8	8	1.97	Useful

3.2. Precipitation Concentration Index (PCI)

The mean annual and seasonal PCI values are presented in Figure 2a–c. Figure 2a shows complex spatial patterns of the annual average PCI values across the Sudano-Sahelian region, which varies from values lower than 20 in the south to higher than 25 in the far north-eastern. In addition, the lowest PCI values are observed in the southern part, ranging from 15 to 20, which is a characteristic of seasonality. While, in the central and far north part of the study area, ranging from 20 to 25 suggests that these areas have strong seasonal precipitation distribution throughout the year (Figure 2a). However, we detected a general increase in PCI values in most stations (Table 4). Thus, significant increases in precipitation concentration values were found mainly in the Fignole, Bidzar, Garoua, Guetale, Madingrin, and Yagoua stations in all parts of the study area. This result indicates that the intra-annual distribution of rainfall is becoming less heterogeneous in the

Sudano-Sahelian region and denotes heavy rainfall falling within a few months throughout the study period.
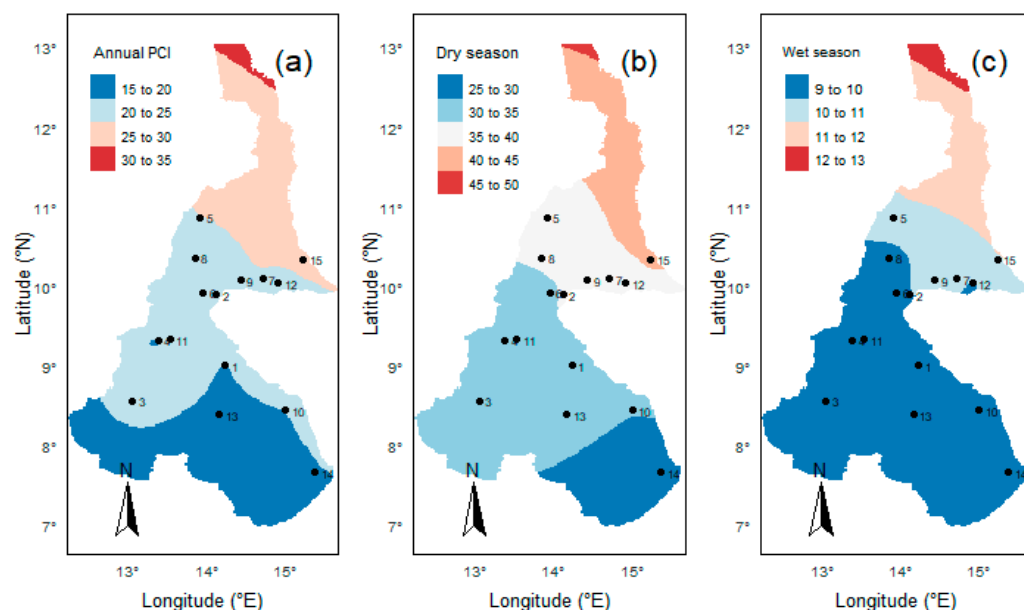
Figure 2. Spatial map of the mean value of (**a**) the annual precipitation concentration index (PCI), (**b**) dry season PCI_{dry}, and (**c**) rainy season PCI_{wet} in the Sudano-Sahelian region of Cameroon.

During the dry season, the spatial pattern demonstrated strong irregular rainfall distribution with a PCI value > 20 in the study area (Figure 2b). For the wet season, rainfall was generally uniformly distributed over a 39-year period, analyzed as having moderate concentrations with PCI < 15, as shown in Figure 2c. In general, similar to the annual PCI, the spatial map of seasonal PCI shows a clear south (lower) to the north gradient (higher). Similar studies in regions such as Ethiopia, [42], Spain [36], and China [43] all point to the fact that seasonal variation associated with more precipitation has a lower PCI value and inversely.

Table 4. Innovative trend analysis (ITA) slopes for PCI, PCD, and PCP. Significant changes (i.e., at the 90% level) are indicated in bold.

| Stations	PCI	PCD	PCP
Bere	0.09	0.0012	0.006
Bidzar	**0.15**	0.0017	0.006
Fignole	**0.23**	0.0026	0.008
Garoua	**0.11**	0.0020	0.005
Guetale	**0.20**	0.0014	0.003
Guider	0.05	0.0006	−0.004
Guidiguis	0.06	0.0011	−0.0003
Hina-Marbak	0.09	0.0011	0.007
Kaélé	0.08	0.0001	0.003
Madingring	**0.11**	0.0020	0.005
Pitoa	0.10	0.0015	−0.001
Tchatibali	0.11	0.0013	0.009
Tchollire	0.08	0.0016	0.004
Touboro	0.05	0.0023	0.01
Yagoua	**0.16**	0.0001	0.011

3.3. Variability of PCD and PCP

Figure 3a,b illustrate the spatial distributions of PCD and PCP values, respectively, over the study area from 1980 to 2018. PCD values ranged from a minimum of 0.65 in the south-eastern part to a maximum of 0.85 in the far north of Cameroon. Most of the climate stations in the Sudano Sahelian region have also exhibited a non-significant increasing trend at the 90% level of PCD, although the slope trend varies between 0.0001/year at Tchollire and Tchatibali in the southern part and 0.0025/year at Guetale in the far north (Table 4). These results indicate that the annual rainy days in a year decreased from the south to the far north, implying a higher probability of flood events in a year toward the far north than in other parts of the Sudano-Sahelian region of Cameroon (Figure 3a).

Mean PCP ranged from a minimum of 7.36 in Guetale to a maximum of 7.50 in Touboro and Tchatibali, which implied that annual rainfall mainly fell in July. The finding indicates that the wet season arrived earlier in the central and far north regions of the study area. The trend directions of PCP showed increasing trends for 12 out of 15 stations, with only three sites (Hina-Marbak, Kaélé, and Yagoua) decreasing at the 90% level. This indicates that the rainy season exhibited a very slight temporal change in an increasing direction over the period 1980–2018, implying a slightly later occurrence of precipitation (Figure 3b).

PCD and PCP are in good agreement with the results of many studies examining the rainfall metrics in the wet season (onset and cessation of the wet season, number of rainy days) in and around the Sahel regions. For example, [19] analyzed the spatial patterns of seasonal rainfall metrics over the period 2000–2015. They found a clear north–south gradient was observed for the onset date and rainy days (RD). Another study was conducted by [9]. They examined the climate–yield relationships in 28 administrative units in north Cameroon. They found that the center of north Cameroon is the most productive area and had the wettest conditions in June.
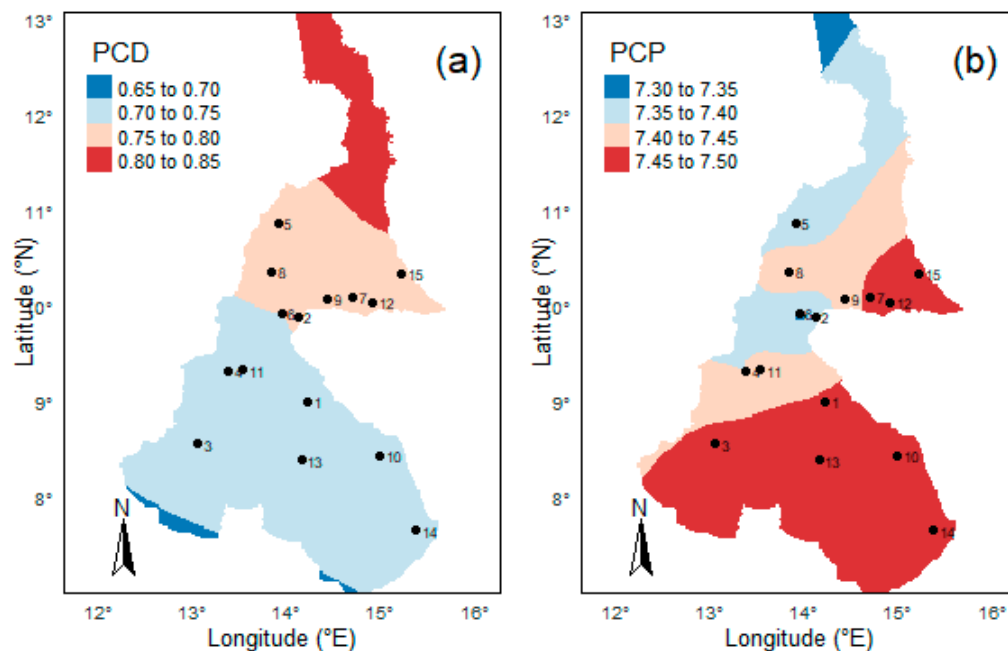
Figure 3. Spatial distribution of the mean annual values for variability parameters from 1980 to 2018. (**a**) Precipitation concentration degree (PCD), and (**b**) Precipitation concentration period (PCP).

3.4. Trend and Magnitude of Extreme Precipitation Events

3.4.1. Intensity Indices

Figures 4–9 shown the intensity indices on the overall and partial trends during 1980–2018. From Figures 4–7, it can be seen that PRCPTOT, SDII, Rx1day, and Rx5day exhibited neutral behaviors at most stations in the study region.

The increase was more evident in Touboro at a rate of 8.5 mm/year and Guetale, Pitoa, and Tchollire stations at a rate of >0.07 mm/day/year, distributed over the entire study area in PRCPTOT and SDII, respectively. In the same direction, the authors of [44] reported both an increase in the total annual rainfall and in the frequency of rainy days, which contributed to partial rainfall recovery in the Sahel. Several studies have justified the increasing rainfall trend over the last three decades via a recovery from the 1970–1980 droughts in West Africa in general [10,45,46]. In general, an increase of low- and medium- value subgroups trends of PRCPTOT and SDII were observed, with the significant stations being Guidiguis, Tchollire, and Touboro, and Fignole, Guetale, Pitoa, and Tchollire, respectively. Regarding, the high-value clusters, significant decreases were noticed, respectively, in PRCPTOT and SDII at Bidzar, Fignole, and Pitoa, and Bidzar and Kaélé stations (Figures 4 and 5); Touboro trended significantly upward in PRCPTOT.

The Garoua, Madingring, and Yagoua and Bere, Garoua, Guetale, Kaélé, and Tchatibali stations appeared to have experienced significant increases at a rate of >0.49 and 0.53 mm/year with Rx1day and Rx5day, respectively (Figures 6 and 7). Whereas, regarding sub-trend interpretations, 'low and medium' depicted the significant increases, respectively, for four and eight stations in Rx1day (Garoua, Madingrin, Tchatibali, and Touboro) and in Rx5day (Bere, Garoua, Guetale, Hina-Marbak, Guidiguis, Tchatibali, Touboro, and Yagoua). Increasing trends were mainly obtained for high Rx1day and Rx5day clusters at Garoua, Guidiguis, Hina-Marbak, Pitoa, and Yagoua and Bidzar, Guidiguis, Kaélé, and Yagoua, respectively. Although decreasing trends were recorded for four to five stations in Rx1day (Bere, Bidzar, Kaélé, Tchatibali, and Tchollire) and in Rx5day (Madingrin, Tchatibali, Tchollire, and Touboro), respectively. Thus, Garoua and Yagoua regions, distributed over the central and southeastern parts of the study area, were manifested both by heavier extreme rainfall. In [23], the authors found similar results to this study, in that the trend of RR1 indicated predominately positive values in the northern part of Cameroon. Among these stations, [47] presented the map of the Maga zone located in the northeast of the study area, in which the Yagoua and Kaélé stations are subjected to flood risks. This increase in extreme daily rainfall suggests an associated increase in intense mesoscale convective systems (MCSs) in the Sudano-Sahelian region [10].

As shown in Figures 8 and 9, on average, R95p and R99p indices show changes in most stations. The significant increasing and decreasing trends of the R95p indices were found in eight (i.e., Bere, Garoua, Guider, Guidiguis, Hina-Marbak, Pitoa, Tchollire, and Touboro) of 1.6–3.12 mm/year and one (i.e., Fignole) of −2.2 mm/year of the fifteen stations in the study area, respectively (Figure 6). Whereas in R99p—seven (i.e., Garoua, Guetale, Hina-Marbak, Madingrin, Pitoa, Tchatibali, and Yagoua) of 0.38–2.82 mm/year and two (i.e., Fignole and Touboro) of −0.98–1.49 mm/year of fifteen stations were observed, respectively (Figure 7). Simultaneously, tendencies for clusters (low and medium) showed that a positive trend was observed in R95p and R99p for most stations. The potential trends in high-value subgroups found that five stations (i.e., Bere, Guidiguis, Pitoa, Tchollire, and Yagoua) experienced significant increases in R95p, and one station (i.e., Guidiguis) in R99p. By contrast, eight stations for R95p (i.e., Bidzar, Fignole, Garoua, Guetale, Guider, Hina-Marbak, Kaélé, and Madingrin) and ten stations (i.e., Bidzar, Fignole, Hina-Marbak, Kaélé, Madingrin, Pitoa, Tchatibali, Touboro, Tchollire, and Yagoua) for R99p displayed significant decreases. Globally, Bere, Pitoa, Guidiguis, Tchollire, and Yagoua stations distributed over parts of the study area, with significant increasing trends in high-value clusters, imply that these percentile-based indices have become more intense in recent decades.
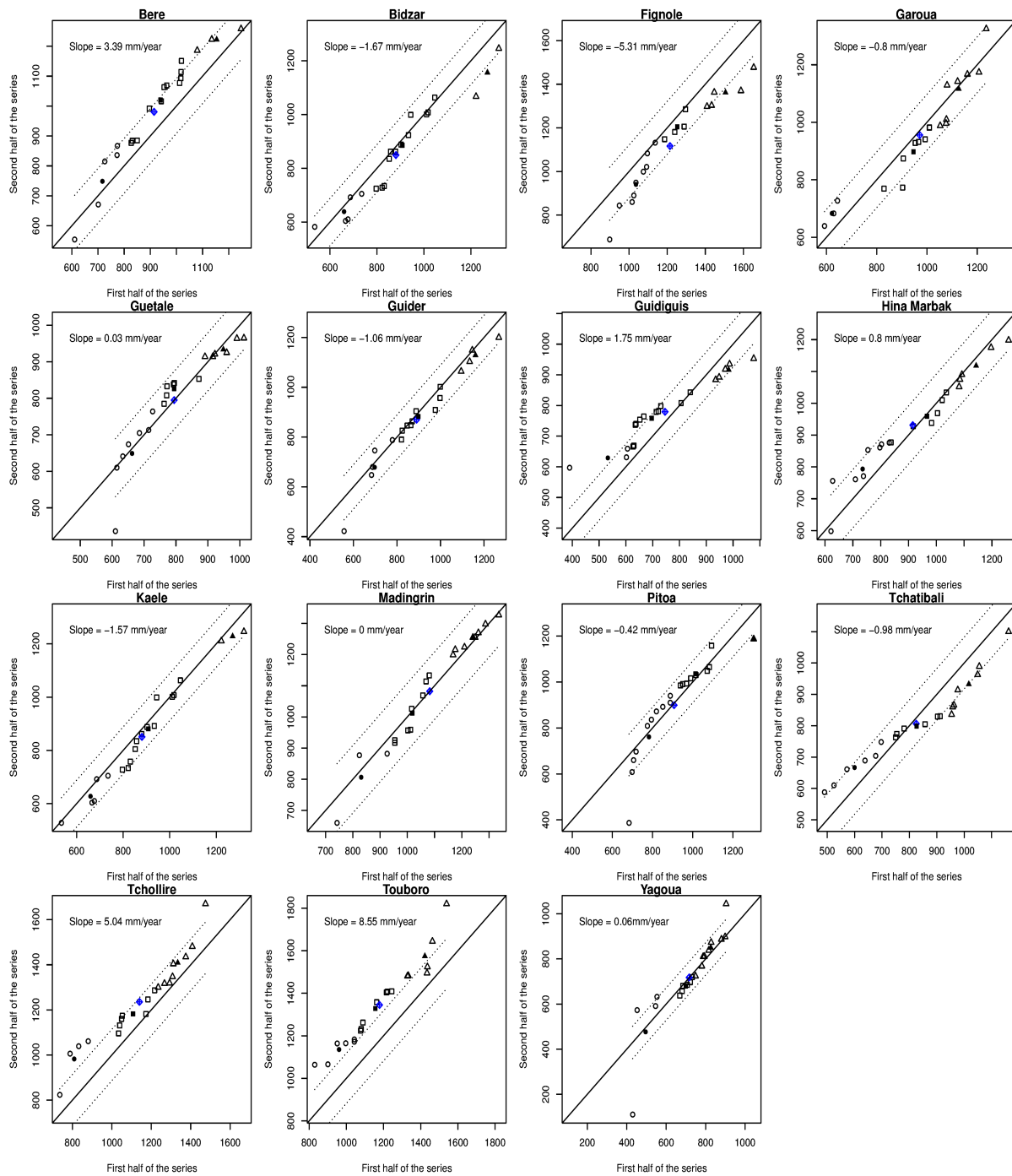
Figure 4. Innovative trend plots for PRCPTOT. The blue diamond symbols indicate monotonic trends over the whole record period, while the gray-filled circle, square, and triangle symbols are mean points of low-, medium-, and high-value clusters, respectively, used for identifying corresponding sub-trends. All random symbols in the upper/lower triangular areas indicate increasing/decreasing trends, while the 1:1 (45°) straight line corresponds to trend-free cases.
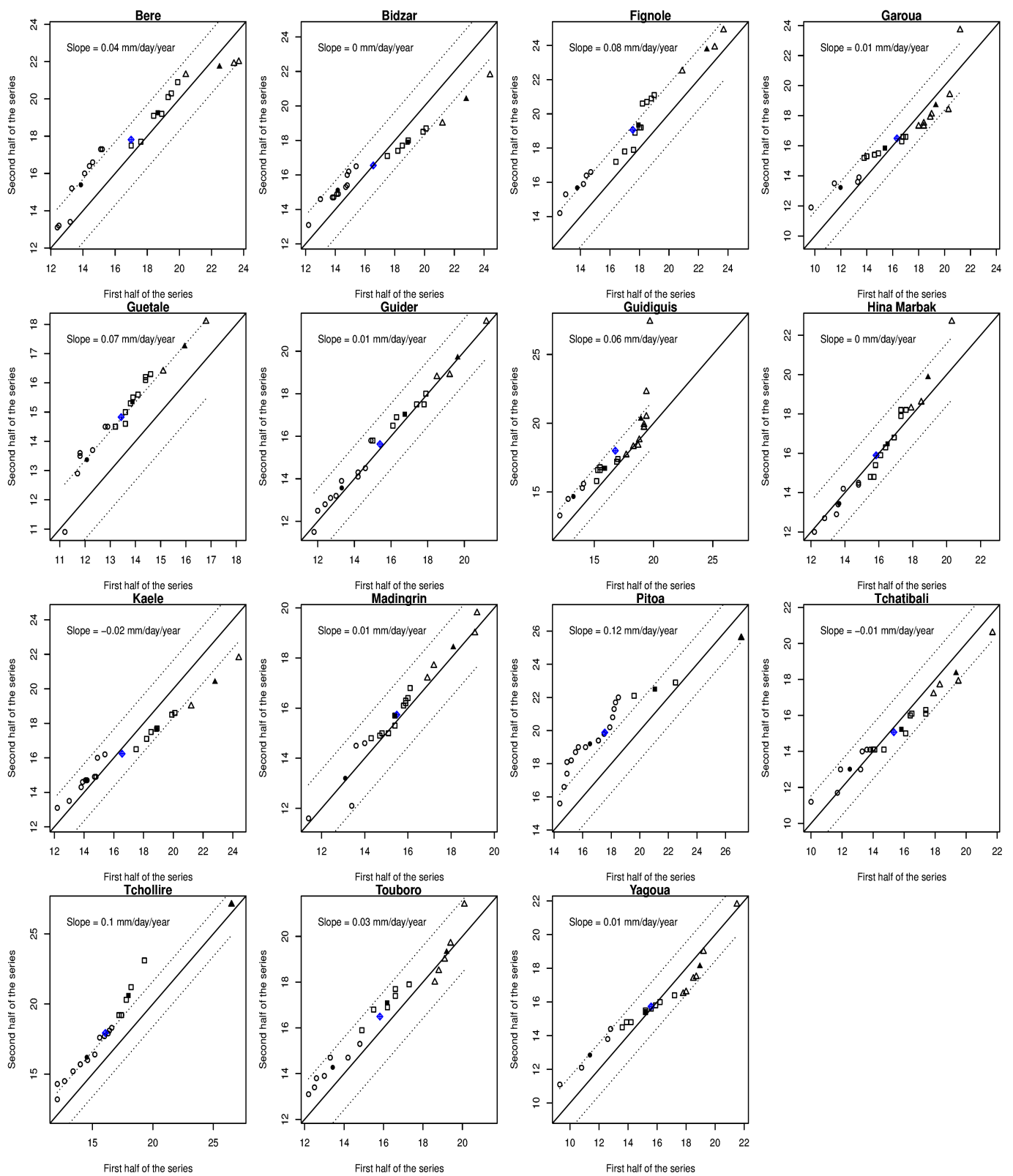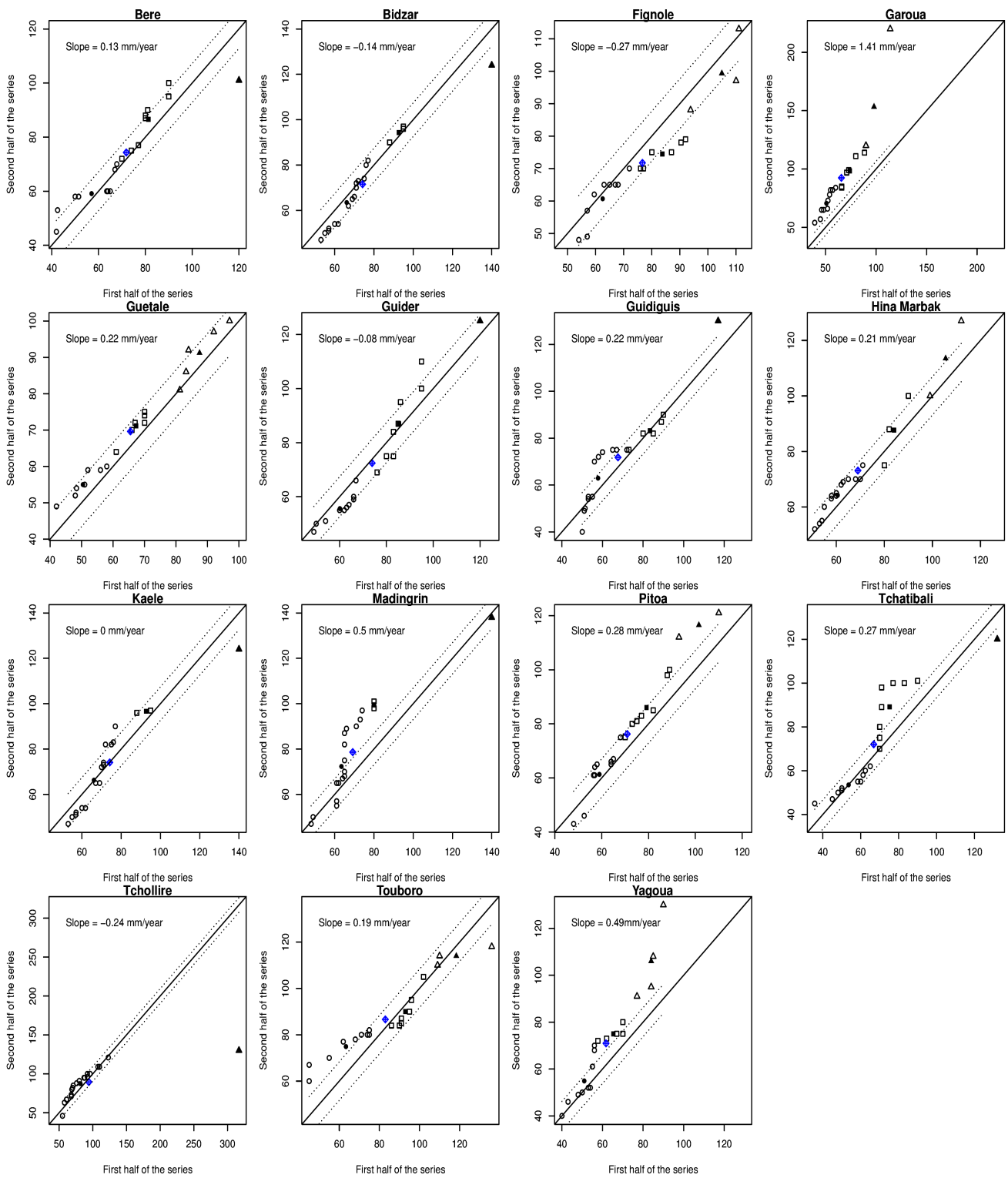
Figure 5. As in Figure 4, but for SDII.
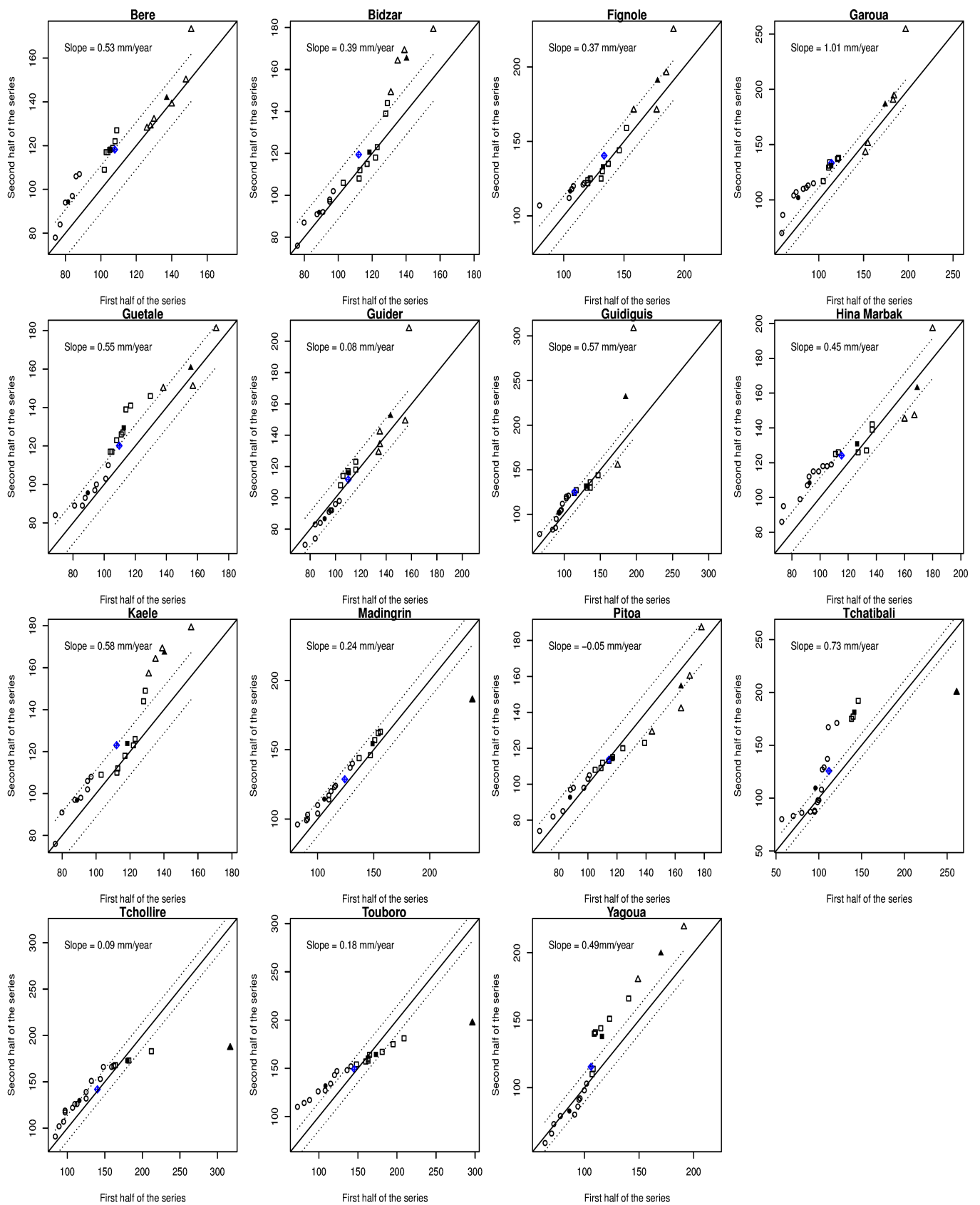
Figure 6. As in Figure 5, but for Rx1day.
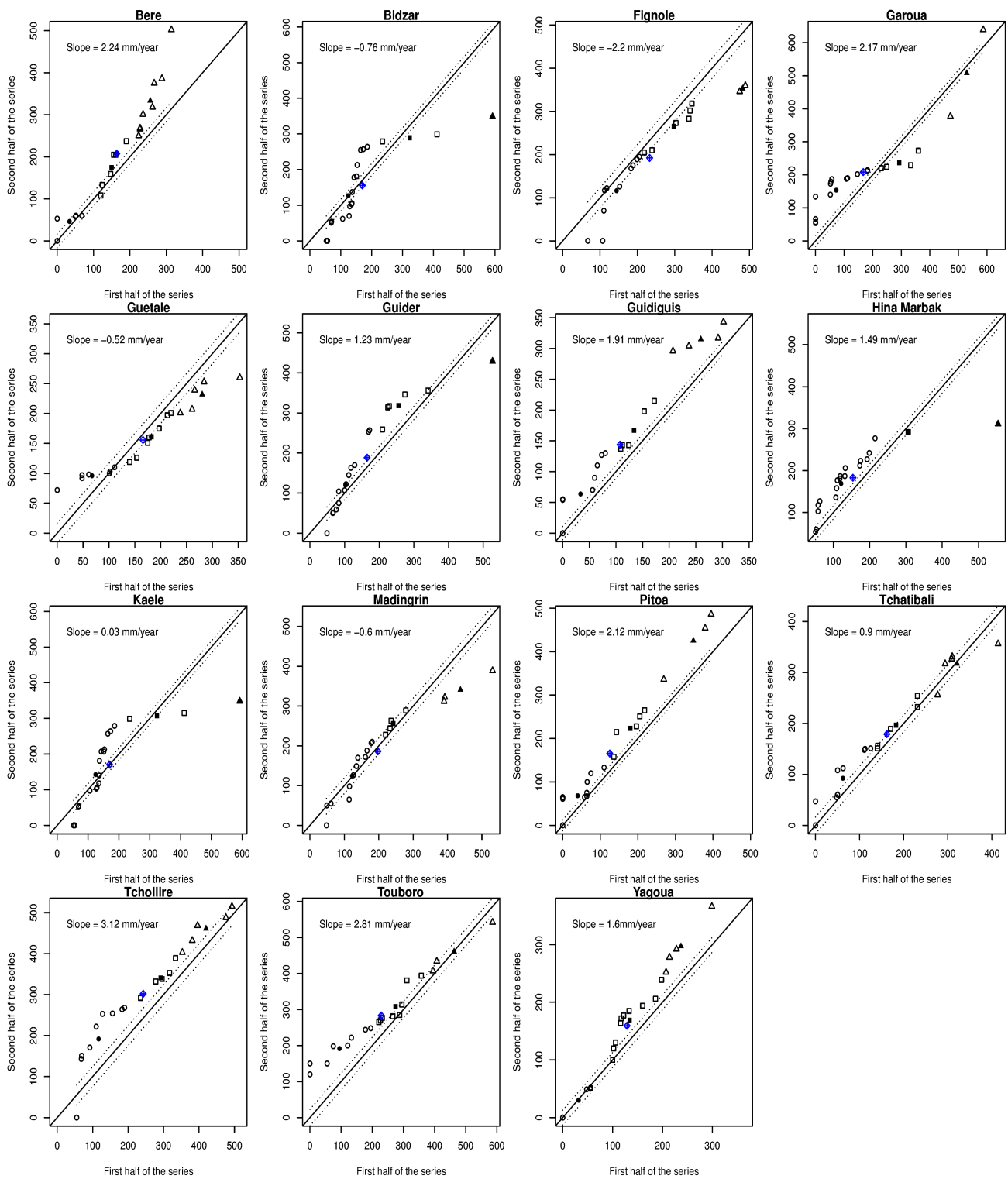
Figure 7. As in Figure 6, but for Rx5day.

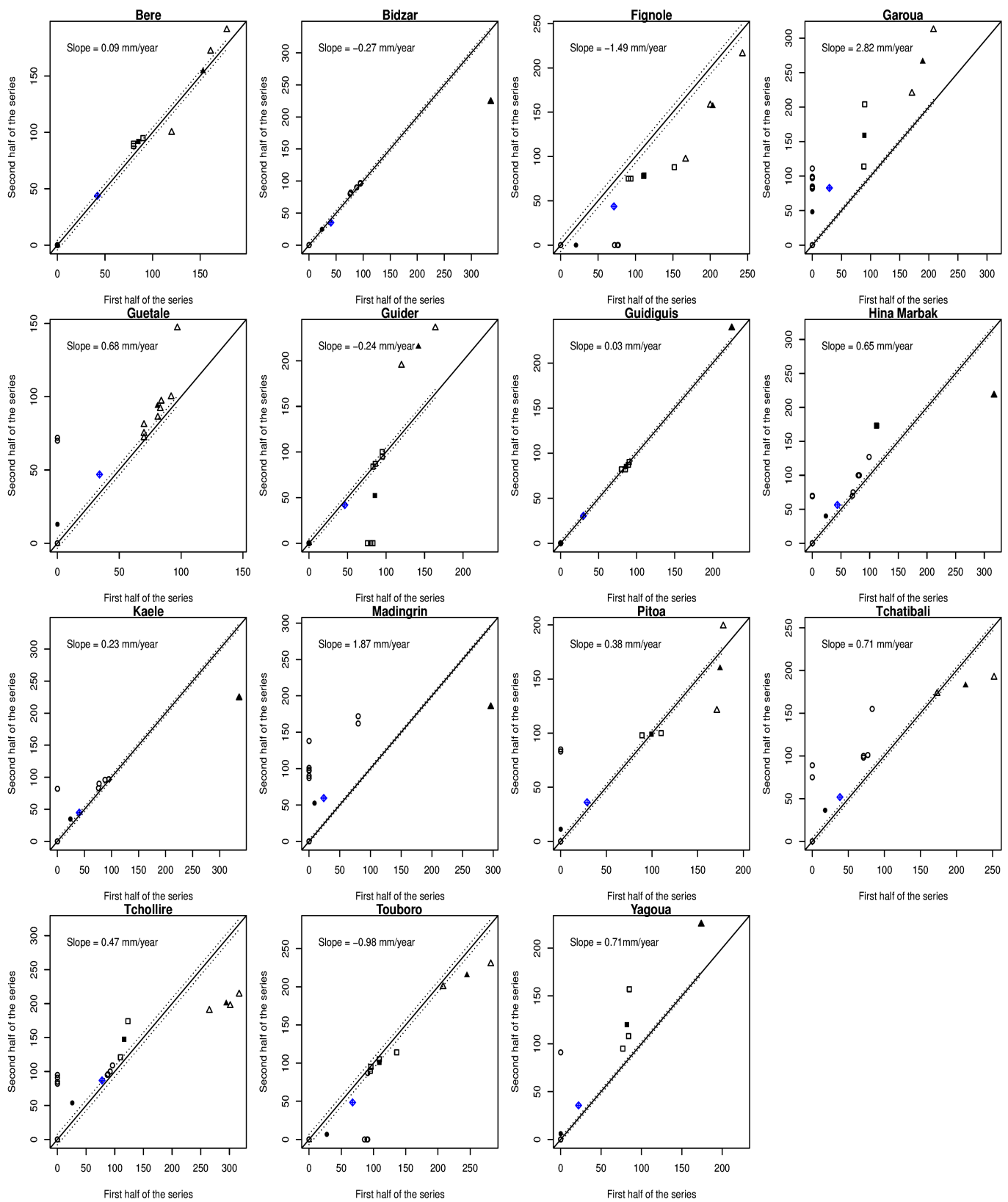**Figure 8.** As in Figure 7, but for R95P.

Figure 9. As in Figure 8, but for R99P.

Results are almost consistent with the results obtained in previous studies at the regional level in West Africa [10,20], Central Africa [48], in the Sahelian region [19,49], and in some nearby areas (for example, Nigeria) [50]. However, the highlights and innovations of this

study identified trends of low, medium, and high values of extreme precipitation in the last forty years; moreover, we compared the monotonic trends in the Sudano-Sahelian zones.

3.4.2. Frequency Indices

Figures 10 and 11 show the indices representing the number of days of extreme rainfall (R10mm and R25mm). In general, trends in R10mm and R25mm have neutral behaviors at most stations. Increasing trends can be observed with only significant trends detected at Touboro at 0.28 days/year and negative at Garoua at −0.21 days/year for R10mm (Figure 10). R25mm values indicate significant increasing trends of 0.06–0.16 days/year at Guetale, Touboro, Bere, and Tchollire stations (Figure 11). The low- and medium clusters were characterized mainly by trend-free behaviors at most stations for R10mm and R25mm. However, for the high-value cluster, Touboro exhibited significant increases in R10mm, and Bere and Touboro—R25mm. Meanwhile, Bidzar, Fignole, Guidiguis, Kaélé, Pitoa, and Tchatibali in R25mm exhibited significant decreases. The general trend is increasing with significant stations, such as Thollire, Bere, and Touboro, located in the southeast of the study area, as shown in Figures 10 and 11. Thus, this part is characterized by more humid days. More recently, [50] demonstrated that this recovery is summarized by a greater number of rainy days associated with a longer duration of the wet period and more extreme rainfall events. This was justified in the central–eastern Sahel in West Africa by the increase in vertical moisture flux, which is mainly driven by the increasing convergence of moisture from remote sources [51].

3.4.3. Duration Indices

The trends of duration indices from 1980 to 2018 over the Sudano-Sahelian are presented in Figures 12 and 13. On average, the CDD trend increased in most of the study area and significantly increased at a rate of 0.88, 0.92, 0.98, 1.02, 1.12, 1.25, and 1.29 days/year in Bere, Garoua, Bidzar, Fignole, Kaélé, Pitoa, and Madingrin stations, respectively (Figure 12). However, no trend was noticed in CWD at most of the stations where the only significant increasing trend was observed in the Touboro station at 0.05 days/year, while stations in Fignole and Pitoa had significant decreasing trends at −0.04 and −0.05 days/year, respectively (Figure 13).

As illustrated in CDD, the Sudano-Sahelian zone mainly experienced increasing trends and low-cluster sequences accounting for 13 stations (except Guetale and Tchollire stations). Simultaneously, Guetale, Madingrin, Pitoa, and Tchollire stations had increasing trends of high-value subgroups.

For the CWD, Bidzar, Fignole, Garoua, Guider, and Kaélé stations indicated increasing trends in high-value subgroups, whereas Yagoua, Tchollire, Pitoa, Madingrin, and Guidiguis experienced significant decreasing trends. At the same time, there were medium-value CWD increasing and decreasing trends; 2 stations (i.e., Touboro and Yagoua) had increasing trends; 4 stations (i.e., Fignole, Guidiguis, Hina-Marbak, and Pitoa) experienced decreasing trends. CDD and CWD indices are indicators of dry climate extremes. Thus, with the significant increasing trend in CDD and decreasing trend in CWD values, Pitoa and Fignole stations localized, respectively, in central and southeast parts of the study area, were the most drought-prone stations. In accordance with the current findings, [52] also indicated extreme droughts occurring in the central and southwestern parts of the area with high frequency.
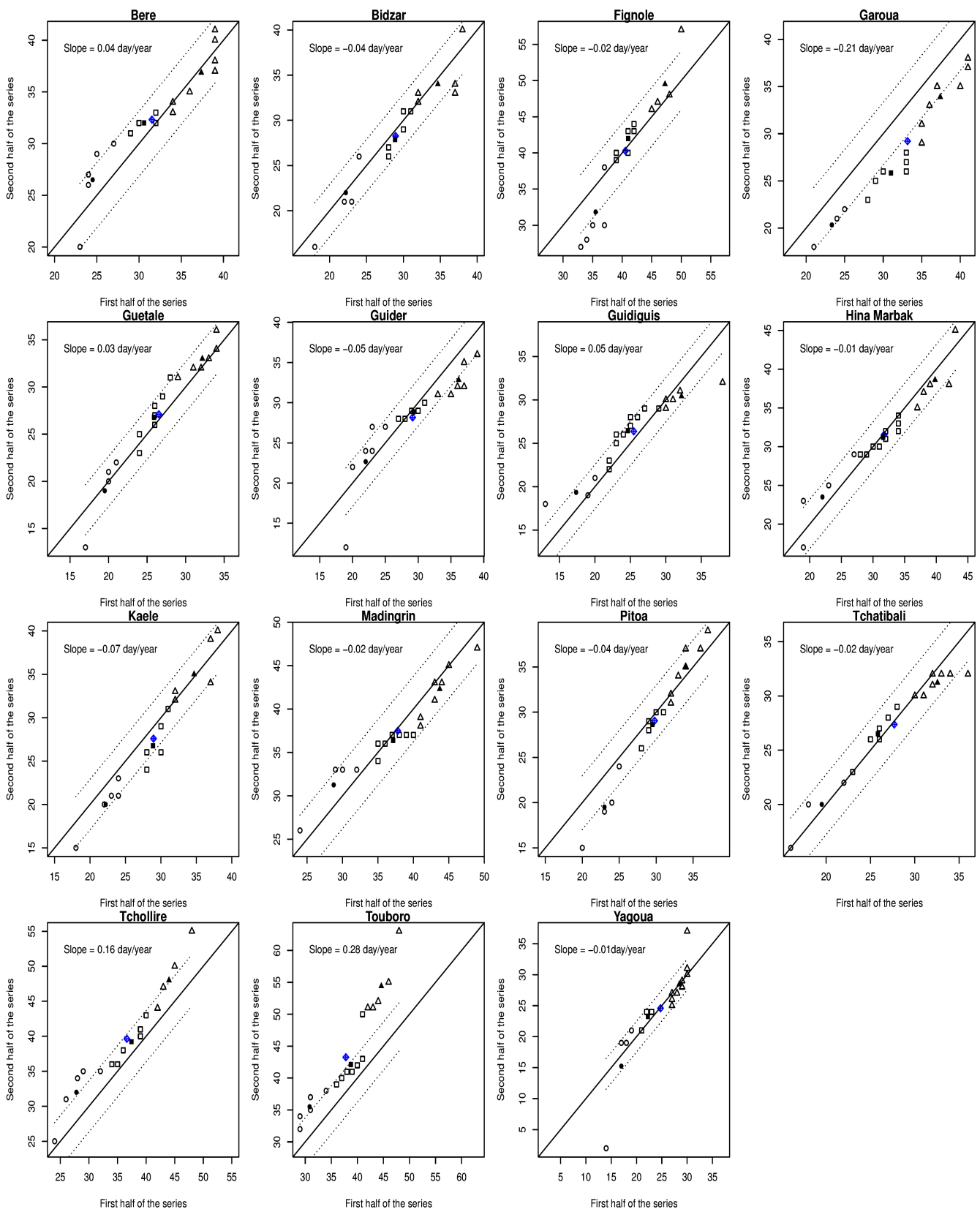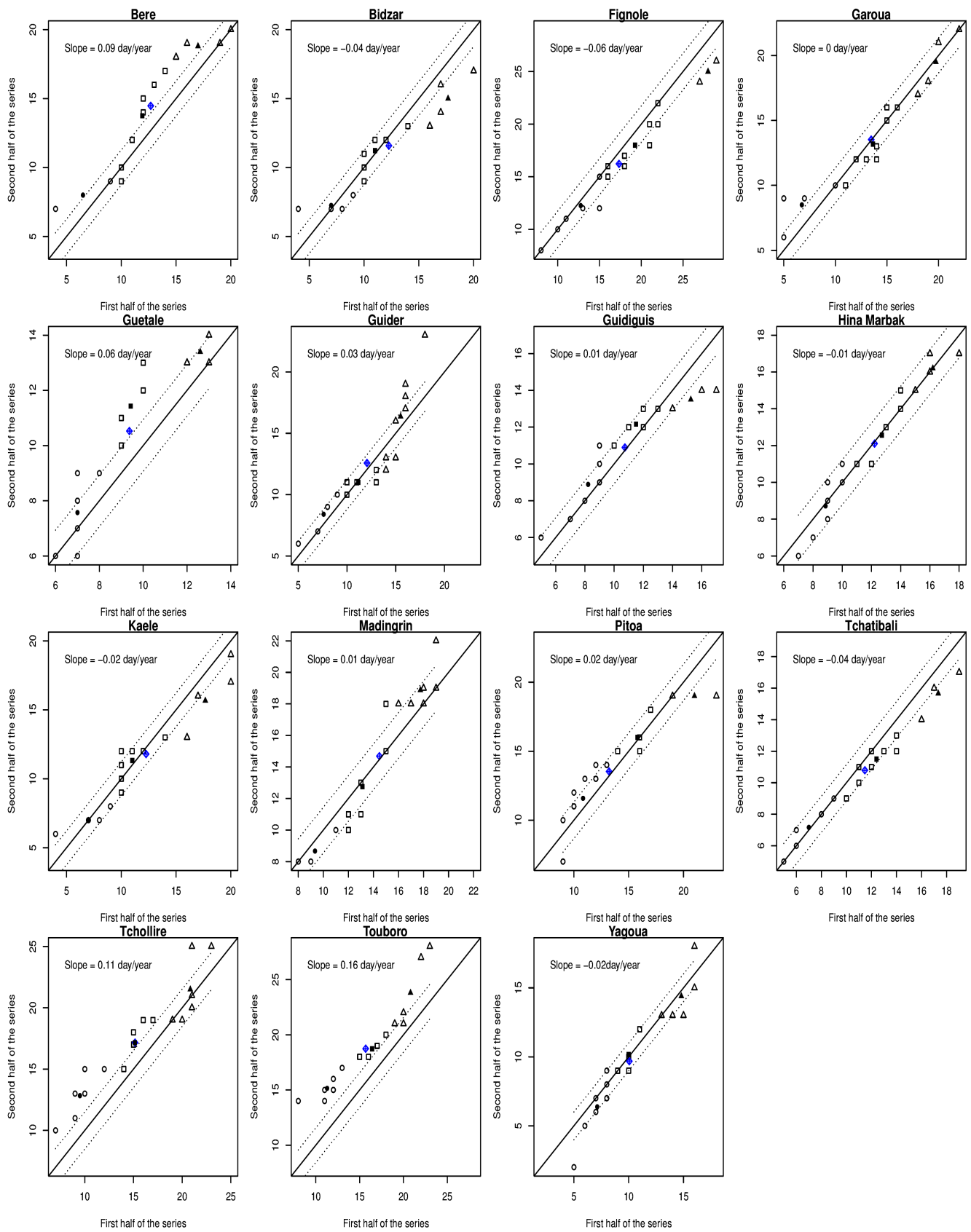
Figure 10. As in Figure 9, but for R10mm.

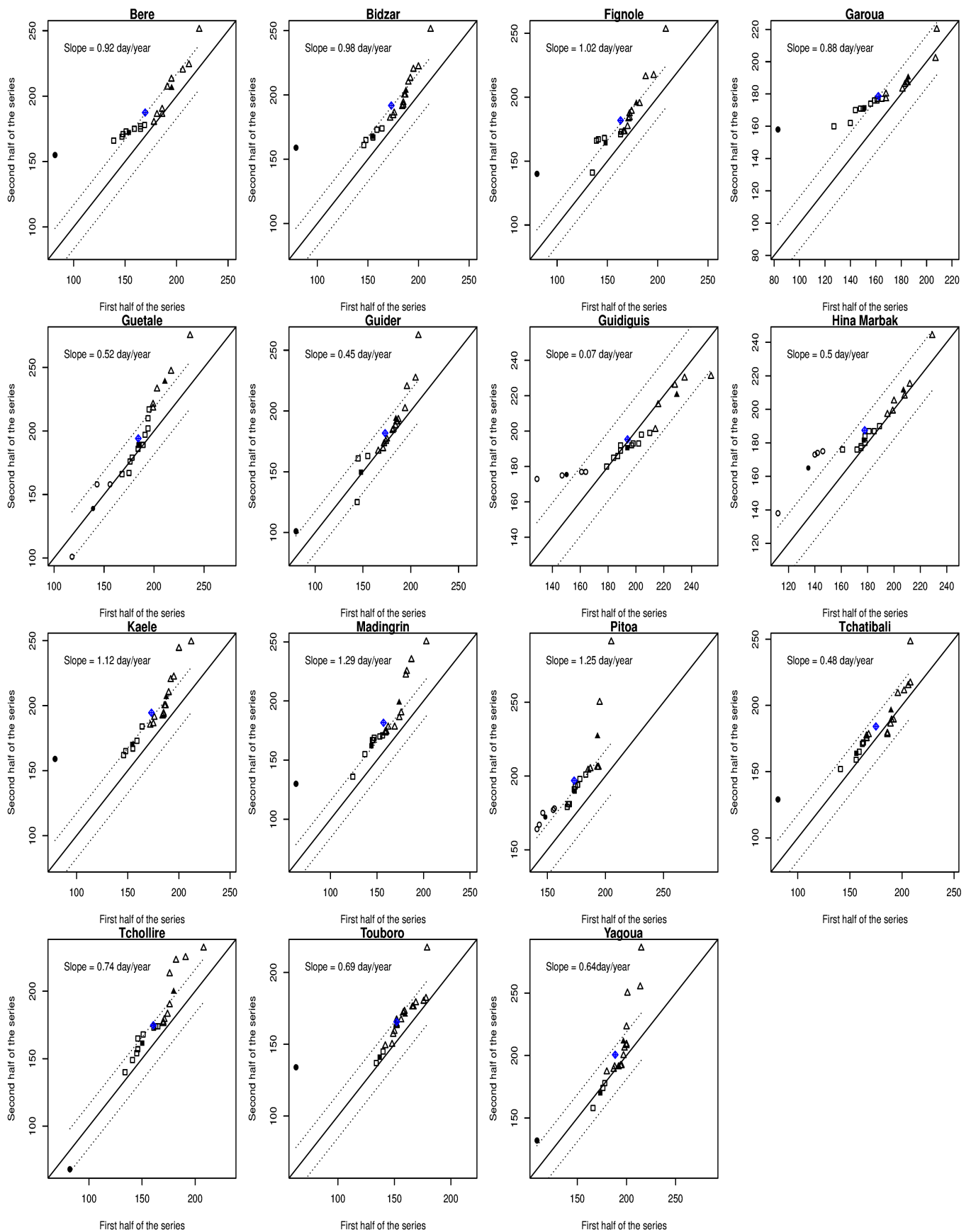**Figure 11.** As in Figure 10, but for R25mm.
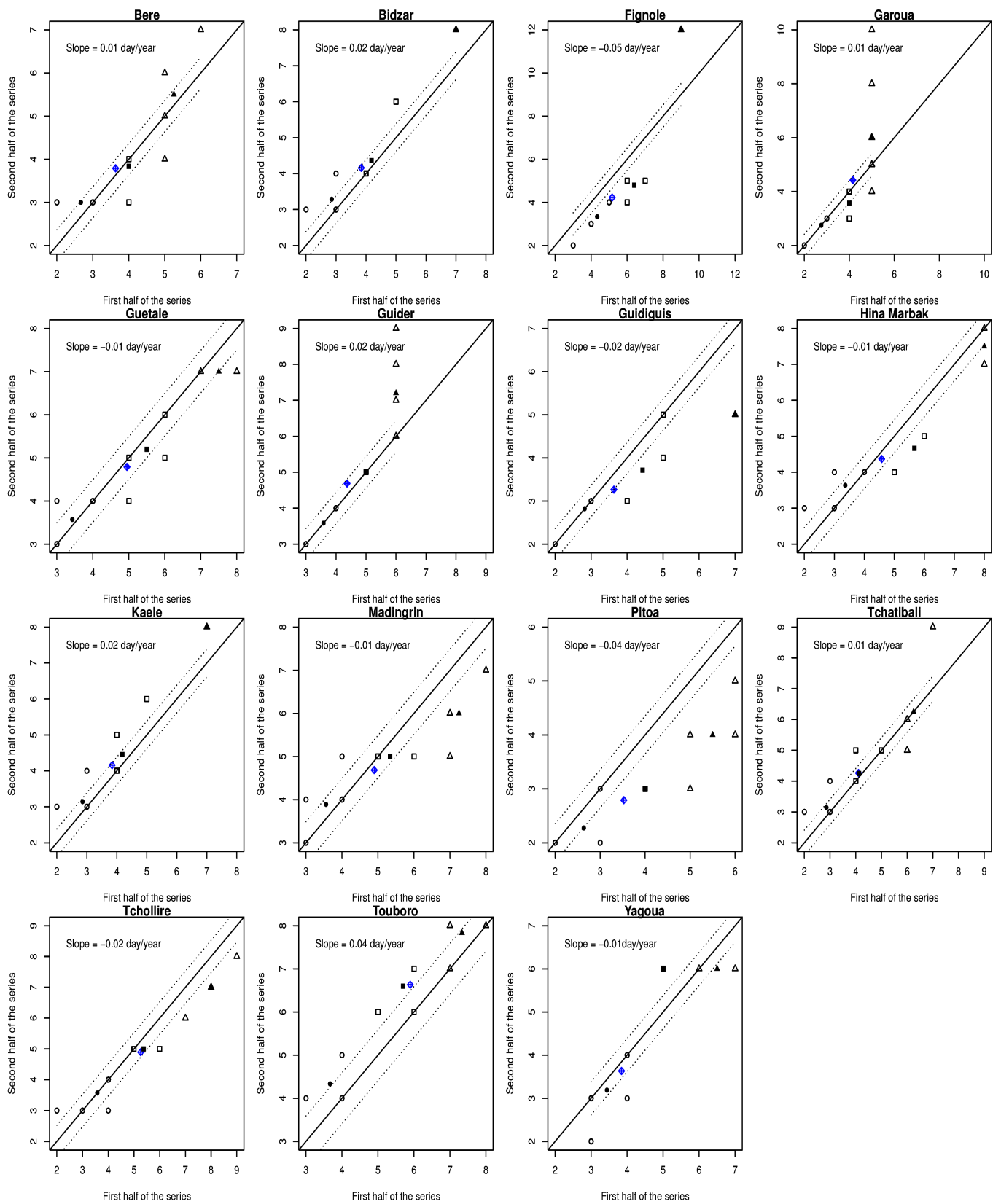
Figure 12. As in Figure 11, but for CDD.

Figure 13. As in Figure 12, but for CWD.

4. Potential Impacts of Climate Variability and Extreme Precipitation on Agriculture and Water Management

Overall, the Sudano-Sahelian region of Cameroon from 1980 to 2018 recorded significant upward trends in extreme rainfall indices (except CWD) in our analysis, such as interannual variability. They were related to the increase in extreme rainfall days. Rainfall during the rainy season was almost uniform, with low PCI levels and a low risk of crop failure, but the amount and distribution of rainfall during this period with late rainfall onset dates indicated by significant increases in PCP impacted some crops and varieties and, thus, crop production and productivity. For instance, [9] found that the rainfall parameters (rainy season onset and length) were major drivers for year-to-year and their variability impacted crop productivity. In addition, heavy rainfall can negatively impact crop yields [53] and cause increased soil erosion. For example, as mentioned in the introduction, the floods in September 2012 in Maga and Yagoua, led to more than 14,000 hectares of crops and 12,375 fruit plants being destroyed (Ministry of Agriculture and Rural Development, 2012).

The study area is mainly drained by four streams—Benue, Chari, Faro, and Logone. They extend to Chad, Nigeria, and RCA. Hence, the high value of annual PCI was observed over the same time period throughout the study area and could cause a challenge for water resource management. Increasing rainfall could favor hydropower production around the Lagdo Dam and increase the supply of drinking water for industrial and domestic uses in the study area. Nevertheless, an increase in daily extreme precipitation (R1xday, R5xday, R95p, and R99p) indices could potentially lead to a greater probability of flooding. From 2010 to 2012, disastrous floods occurred in Yagoua and Guirvidig in the south-eastern part of the study area, as in many Sahelian countries, resulting in the destruction of the dike, many deaths, and material losses [47,54]. On the other hand, as an indicator of the lack of rainfall, an increase in CDD and a decrease in CWD could create challenging situations for agricultural practices, food security, and runoff from major rivers.

5. Conclusions

This study analyzed spatiotemporal variability and changes in mean rainfall and extreme indices in the Sudano-Sahelian region of Cameroon based on daily synoptic rainfall datasets for the period from 1980 to 2018. A homogeneity test was performed on the data series using the standard normal homogeneity test (SNHT), the Pettitt test, the Buishand range test, and the Von Neumann ratio test. The ETCCDI (Expert Team on Climate Change Detection Indices) indices were calculated using RClimDex version 1.0 software. These climate indices were used to assess corresponding trends in the frequency and intensity of daily rainfall. Based on the Sen slope and the innovative trend analysis (ITA), most of the rainfall stations showed statistically significant upward trends for annual rainfall. The temporal and spatial variability of precipitation using the precipitation concentration index (PCI), precipitation concentration period (PCP), and the precipitation concentration degree (PCD) showed higher variabilities of precipitation for the annual and dry season scales than the wet seasons. Most stations showed significant increasing trends in the number of very heavy rains and precipitation intensity indices. In addition, a significant increase was observed for consecutive dry days (CDD) in the study area while the opposite trends were observed for consecutive wet days (CWD), so very few were significant. However, this study highlights further research on how the hydrological regime responds to climate change, causing flooding, food insecurity, and affecting water resources in the Sudano-Sahelian zones. It is beneficial for the future social and economic planning of the country and the sub-region. In future studies, the relationship between African Monsoon variation and extreme rainfall events in the study area should be further investigated.

Author Contributions: All authors contributed to the study conception and design. I.N., L.A.D.T., B.O.A., G.M.G., D.A.V. and R.N. contributed to the conceptualization of the study. The first draft of the manuscript was written by I.N. and all authors commented on previous versions of the manuscript. All authors have read and agreed to the published version of the manuscript.

References

1. Nicholson, S.E. The nature of rainfall variability over Africa on time scales of decades to millenia. *Glob. Planet. Chang.* **2000**, *26*, 137–158. [CrossRef]
2. Leisinger, K.M.; Schmitt, K. *Survival in the Sahel: An Ecological and Developmental Challenge*; International Service for National Agricultural Research (ISNAR): The Hague, The Netherlands, 1995.
3. Kharin, V.V.; Zwiers, F.W.; Zhang, X.; Hegerl, G.C. Changes in Temperature and Precipitation Extremes in the IPCC Ensemble of Global Coupled Model Simulations. *J. Clim.* **2007**, *20*, 1419–1444. [CrossRef]
4. Field, C.B.; Barros, V.; Stocker, T.F.; Dahe, Q. *Managing the Risks of Extreme Events and Disasters to Advance Climate Change Adaptation: Special Report of the Intergovernmental Panel on Climate Change*; Cambridge University Press: Cambridge, UK, 2012.
5. Fischer, E.M.; Beyerle, U.; Knutti, R. Robust spatially aggregated projections of climate extremes. *Nat. Clim. Chang.* **2013**, *3*, 1033–1038. [CrossRef]
6. Taylor, C.; Belušić, D.; Guichard, F.; Parker, D.; Vischel, T.; Bock, O.; Harris, P.; Janicot, S.; Klein, C.; Panthou, G. Frequency of extreme Sahelian storms tripled since 1982 in satellite observations. *Nature* **2017**, *544*, 475–478. [CrossRef] [PubMed]
7. Niasse, M. *Reducing West Africa's Vulnerability to Climate Impacts on Water Resources, Wetlands and Desertification: Elements for a Regional Strategy for Preparedness and Adaptation*; IUCN: Gland, Switzerland, 2004.
8. Berg, A.; Quirion, P.; Sultan, B. Weather-Index Drought Insurance in Burkina-Faso: Assessment of Its Potential Interest to Farmers. *Weather. Clim. Soc.* **2009**, *1*, 71–84. [CrossRef]
9. Sultan, B.; Bella-Medjo, M.; Berg, A.; Quirion, P.; Janicot, S. Multi-scales and multi-sites analyses of the role of rainfall in cotton yields in West Africa. *Int. J. Climatol.* **2009**, *30*, 58–71. [CrossRef]
10. Sanogo, S.; Fink, A.H.; Omotosho, J.A.; Ba, A.; Redl, R.; Ermert, V. Spatio-temporal characteristics of the recent rainfall recovery in West Africa. *Int. J. Climatol.* **2015**, *35*, 4589–4605. [CrossRef]
11. Molua, E.L.; Lambi, C.M. *The Economic Impact of Climate Change on Agriculture in Cameroon*; World Bank Policy Research Working Paper; World Bank Group: Washington, DC, USA, 2007; Volume 1. [CrossRef]
12. INS. *Rapport National sur les Objectifs du Millénaire pour le Développement en 2015. Édit*; Institut National de la Statistique: Yaoundé, Cameroun, 2015; 48p.
13. DSCN. *Conditions de vie des Ménages et Profil de Pauvreté à L'extrême-Nord Cameroun en 2001. Édit*; Étude Réalisée Dans la Cadre du Prepafen; Direction de la Statistique et de la Comptabilité Nationale: Yaoundé, Cameroon, 2002; 131p.
14. Kamga, F.M. Impact of greenhouse gas induced climate change on the runoff of the Upper Benue River (Cameroon). *J. Hydrol.* **2001**, *252*, 145–156. [CrossRef]
15. MINEPDED. Les Conditions et les Stratégies de Lutte Contre la Sécheresse au Cameroun. 2016. Available online: https://www.droughtmanagement.info/wp-content/uploads/2016/10/WS6-CAMEROON.pdf (accessed on 28 September 2022).
16. Igri, P.M.; Tanessong, R.S.; Vondou, D.A.; Mkankam, F.K.; Panda, J. Added-Value of 3DVAR Data Assimilation in the Simulation of Heavy Rainfall Events Over West and Central Africa. *Pure Appl. Geophys.* **2015**, *172*, 2751–2776. [CrossRef]
17. Igri, P.M.; Tanessong, R.S.; Vondou, D.A.; Panda, J.; Garba, A.; Mkankam, F.K.; Kamga, A. Assessing the performance of WRF model in predicting high-impact weather conditions over Central and Western Africa: An ensemble-based approach. *Nat. Hazards* **2018**, *93*, 1565–1587. [CrossRef]
18. Cheo, A.E.; Voigt, H.-J.; Mbua, R.L. Vulnerability of water resources in northern Cameroon in the context of climate change. *Environ. Earth Sci.* **2013**, *70*, 1211–1217. [CrossRef]
19. Zhang, W.; Brandt, M.; Tong, X.; Tian, Q.; Fensholt, R. Impacts of the seasonal distribution of rainfall on vegetation productivity across the Sahel. *Biogeosciences* **2018**, *15*, 319–330. [CrossRef]
20. Barry, A.A.; Caesar, J.; Tank, A.M.G.K.; Aguilar, E.; McSweeney, C.; Cyrille, A.M.; Nikiema, M.P.; Narcisse, K.B.; Sima, F.; Stafford, G.; et al. West Africa climate extremes and climate change indices. *Int. J. Climatol.* **2018**, *38*, e921–e938. [CrossRef]
21. Fotso-Nguemo, T.C.; Chamani, R.; Yepdo, Z.D.; Sonkoué, D.; Matsaguim, C.N.; Vondou, D.A.; Tanessong, R.S. Projected trends of extreme rainfall events from CMIP5 models over Central Africa. *Atmos. Sci. Lett.* **2018**, *19*, e803. [CrossRef]
22. Dassou, E.F.; Ombolo, A.; Chouto, S.; Mboudou, G.E.; Essi, J.M.A.; Bineli, E. Trends and Geostatistical Interpolation of Spatio-Temporal Variability of Precipitation in Northern Cameroon. *Am. J. Clim. Chang.* **2016**, *5*, 229–244. [CrossRef]
23. Vondou, D.; Guenang, G.; Djiotang, T.; Kamsu-Tamo, P. Trends and Interannual Variability of Extreme Rainfall Indices over Cameroon. *Sustainability* **2021**, *13*, 6803. [CrossRef]

24. Şen, Z. Innovative trend analysis methodology. *J. Hydrol. Eng.* **2012**, *17*, 1042–1046. [CrossRef]

25. Şen, Z. Trend identification simulation and application. *J. Hydrol. Eng.* **2014**, *19*, 635–642. [CrossRef]

26. Şen, Z. Innovative trend significance test and applications. *Theor. Appl. Climatol.* **2017**, *127*, 939–947. [CrossRef]

27. Mallick, J.; Talukdar, S.; Alsubih, M.; Salam, R.; Ahmed, M.; Ben Kahla, N. Shamimuzzaman Analysing the trend of rainfall in Asir region of Saudi Arabia using the family of Mann-Kendall tests, innovative trend analysis, and detrended fluctuation analysis. *Theor. Appl. Climatol.* **2020**, *143*, 823–841. [CrossRef]

28. Mann, H.B. Nonparametric tests against trend. *Econometrica* **1945**, *13*, 245–259. [CrossRef]

29. Kendall, M.G. *Rank Correlation Methods*; Charles Griffin: London, UK, 1955.

30. Penlap, E.; Matulla, C.; von Storch, H.; Kamga, F. Downscaling of GCM scenarios to assess precipitation changes in the little rainy season (March–June) in Cameroon. *Clim. Res.* **2004**, *26*, 85–96. [CrossRef]

31. Alexandersson, H. A homogeneity test applied to precipitation data. *J. Climatol.* **1986**, *6*, 661–675. [CrossRef]

32. Buishand, T. Some methods for testing the homogeneity of rainfall records. *J. Hydrol.* **1982**, *58*, 11–27. [CrossRef]

33. Pettitt, A.N. A Non-Parametric Approach to the Change-Point Problem. *Appl. Stat.* **1979**, *28*, 126–135. [CrossRef]

34. Von Neumann, J. Distribution of the Ratio of the Mean Square Successive Difference to the Variance. *Ann. Math. Stat.* **1941**, *12*, 367–395. [CrossRef]

35. Wijngaard, J.B.; Tank, A.M.G.K.; Können, G.P. Homogeneity of 20th century European daily temperature and precipitation series. *Int. J. Climatol.* **2003**, *23*, 679–692. [CrossRef]

36. De Luis, M.; González-Hidalgo, J.C.; Brunetti, M.; Longares, L.A. Precipitation concentration changes in Spain 1946–2005. *Nat. Hazards Earth Syst. Sci.* **2011**, *11*, 1259–1265. [CrossRef]

37. Oliver, J.E. Monthly Precipitation Distribution: A Comparative Index. *Prof. Geogr.* **1980**, *32*, 300–309. [CrossRef]

38. Zhang, L.; Qian, Y. Annual distribution features of precipitation in China and their interannual variations. *Acta Meteorol. Sin.* **2003**, *17*, 146–163.

39. Zhang, X.; Alexander, L.; Hegerl, G.C.; Jones, P.; Tank, A.K.; Peterson, T.C.; Trewin, B.; Zwiers, F.W. Indices for monitoring changes in extremes based on daily temperature and precipitation data. *Wires Clim. Chang.* **2011**, *2*, 851–870. [CrossRef]

40. Phuong, D.N.D.; Huyen, N.T.; Liem, N.D.; Hong, N.T.; Cuong, D.K.; Loi, N.K. On the use of an innovative trend analysis methodology for temporal trend identification in extreme rainfall indices over the Central Highlands, Vietnam. *Theor. Appl. Climatol.* **2021**, *147*, 835–852. [CrossRef]

41. Djoufack, V.; Fontaine, B.; Martiny, N.; Tsalefac, M. Climatic and demographic determinants of vegetation cover in northern Cameroon. *Int. J. Remote Sens.* **2012**, *33*, 6904–6926. [CrossRef]

42. Shawul, A.A.; Chakma, S. Trend of extreme precipitation indices and analysis of long-term climate variability in the Upper Awash basin, Ethiopia. *Theor. Appl. Climatol.* **2020**, *140*, 635–652. [CrossRef]

43. Zhang, K.; Yao, Y.; Qian, X.; Wang, J. Various characteristics of precipitation concentration index and its cause analysis in China between 1960 and 2016. *Int. J. Climatol.* **2019**, *39*, 4648–4658. [CrossRef]

44. Ibrahim, B.; Karambiri, H.; Polcher, J.; Yacouba, H.; Ribstein, P. Changes in rainfall regime over Burkina Faso under the climate change conditions simulated by 5 regional climate models. *Clim. Dyn.* **2013**, *42*, 1363–1381. [CrossRef]

45. Druyan, L.M. Studies of 21st-century precipitation trends over West Africa. *Int. J. Climatol.* **2010**, *31*, 1415–1424. [CrossRef]

46. Chaney, N.W.; Sheffield, J.; Villarini, G.; Wood, E.F. Development of a High-Resolution Gridded Daily Meteorological Dataset over Sub-Saharan Africa: Spatial Analysis of Trends in Climate Extremes. *J. Clim.* **2014**, *27*, 5815–5835. [CrossRef]

47. Leumbe, O.; Bitom, D.; Mamdem, L.; Tiki, D.; Ibrahim, A. Cartographie des zones à risques d'inondation en zone soudano-sahélienne: Cas de Maga et ses environs dans la région de l'extrême-nord Cameroun. *Afr. Sci. Rev. Int. Sci. Technol.* **2015**, *11*, 45–61.

48. Aguilar, E.; Barry, A.A.; Brunet, M.; Ekang, L.; Fernandes, A.; Massoukina, M.; Mbah, J.; Mhanda, A.; do Nascimento, D.J.; Peterson, T.C.; et al. Changes in temperature and precipitation extremes in western central Africa, Guinea Conakry, and Zimbabwe, 1955–2006. *J. Geophys. Res. Atmos.* **2009**, *114*. [CrossRef]

49. Mouhamed, L.; Traore, S.B.; Alhassane, A.; Sarr, B. Evolution of some observed climate extremes in the West African Sahel. *Weather Clim. Extrem.* **2013**, *1*, 19–25. [CrossRef]

50. Gbode, I.E.; Adeyeri, O.E.; Menang, K.P.; Intsiful, J.D.K.; Ajayi, V.O.; Omotosho, J.A.; Akinsanola, A.A. Observed changes in climate extremes in Nigeria. *Meteorol. Appl.* **2019**, *26*, 642–654. [CrossRef]

51. Akinsanola, A.A.; Zhou, W. Dynamic and thermodynamic factors controlling increasing summer monsoon rainfall over the West African Sahel. *Clim. Dyn.* **2018**, *52*, 4501–4514. [CrossRef]

52. Njouenwet, I.; Vondou, D.A.; Dassou, E.F.; Ayugi, B.O.; Nouayou, R. Assessment of agricultural drought during crop-growing season in the Sudano–Sahelian region of Cameroon. *Nat. Hazards* **2021**, *106*, 561–577. [CrossRef]

53. Njouenwet, I.; Vondou, D.A.; Ashu, S.V.N.; Nouayou, R. Contributions of Seasonal Rainfall to Recent Trends in Cameroon's Cotton Yields. *Sustainability* **2021**, *13*, 12086. [CrossRef]

54. Saha, F.; Tchindjang, M.; Dzana, J.-G.; Nguemadjita, D. Risques naturels dans la région de l'Extrême-Nord du Cameroun et dynamique des extrêmes hydrologiques du système Chari-Logone. *Physio-Géo Géogr. Phys. Environ.* **2020**, *15*, 69–88. [CrossRef]